Superalloys 2004
Edited by K.A. Green, T.M. Pollock, H. Harada,
T.E. Howson, R.C. Reed, J.J. Schirra, and S. Walston
TMS (The Minerals, Metals & Materials Society), 2004

ABNORMAL PHASES IN HIGH W CONTENT NICKEL BASE SUPERALLOYS AND PHASE CONTROL

Yunrong Zheng[1, 2], Shusuo Li[1], Liang Zheng[2, 3], Yafang Han[1, 2]

[1]School of Materials Science and Engineering, Beijing University of Aeronautics and Astronautics, Beijing 100083, China
[2]Beijing Institute of Aeronautical Materials, Beijing 100095, China
[3]School of Materials Science and Engineering, Xi'an University of Technology, Xi'an 710048

Keywords: Die superalloys, Solidification, Phase transformation, Mechanical properties, M_6C carbides, α phase, μ phase

Abstract

In this paper, the forming conditions and harmful effects of the abnormal phases such as M_6C carbides, α (W, Mo) and μ in a series of high W content K9, K20 and 601 alloys, which are suitable for forging die, have been studied. The abnormal phases precipitated from liquid belong to primary phases. The large blocky M_6C formed in as-cast alloys, as the total amount of (W+Mo) and carbon content exceeded 18 wt% and 0.15 wt% respectively, while the carbon content less than 0.06 wt% promoted the formation of primary α and μ phases. The addition of elements such as Co or Ru and the rapid solidification exhibited a decreased tendency to precipitate M_6C carbides. The primary M_6C carbide is the most stable phase among the three abnormal phases and is not removed until the full melting of alloy. Contrarily, the α and μ are unstable phases and can transform to M_6C carbides. The primary M_6C carbides severely deteriorate the mechanical properties of the alloys, and the stress rupture life of the alloys at 1100℃/118MPa decreased over 50%, as the volume fraction of primary M_6C in alloys was higher than 1.5%. It was very difficult to avoid the formation of primary M_6C for a heavy section forging die cast by this series alloys, therefore the compositional modification for these alloys was performed.

Introduction

Conventional highly alloyed cast Ni-base alloys drop off sharply in strength above approximately 1100℃ because the γ' phase, upon which these alloys primarily depend for high temperature strength, agglomerates or goes into solution in this temperature range. The element W is a stabilizer of γ' phase and increases melting temperature, therefore some cast Ni-base superalloys containing 16~19 wt% W were developed in United States in the 1960's to 1970's. The representative alloys were WAZ20 [1], WAZ16 [2] and IN591-X [3]. With the development of superalloys, the content of high cost elements such as Ta and Re was continuously raised in order to improve the temperature capability of the alloys [4, 5], and hence the materials cost increased dramatically [6]. For the high temperature structural materials used for the industrial gas turbine vanes and forging dies, the cost factor is one of the most important considerations in commercial competition.

In China, it was paid attention to develop a series of cast nickel based superalloys K9, K20 and Alloy 601 for potential stator vanes application of gas turbines in the past 30 years. All these alloys contain 14~16 wt% W and belong to (Ta, Re, Hf)-free low cost alloys. Among them the conventional cast Alloy 601 possesses a superior strength corresponding to that of the first generation SC superalloys DD3 at 1100℃ [7] and can meet the cost demand. At present, Alloy K9 has been successfully applied to large size forging dies working in the temperature range of 1050℃ to 1100℃. However, the alloy is very sensitive to the composition limits and cast process. Out of the narrow control range, the abnormal phase characterized by M_6C, μ and α (W, Mo) will appear during solidification [8]. Especially, the large blocky primary M_6C carbides seriously deteriorate the mechanical properties of the alloys. Hence, the systematical investigation on forming conditions and avoidance ways of abnormal phases was carried out to provide technical support for further application of alloys in this study.

Experimental Procedures

Thirteen 5kg-master alloys with 16~22 wt% (W+Mo) were prepared by vacuum induction melting followed by remelting and cast to the shaped test bars. The analysis compositions of these alloys are listed in Table Ⅰ. The Alloy 4, 7 and 9 are denominated as K9, K20 and Alloy 601 respectively. The others are the modified composition alloys for different levels of Co, W, Mo, Ta and C.

In order to explore the forming and transforming conditions of abnormal phases, a part of specimens was heat-treated at 1230~1300℃/0.3~0.4h or thermo-exposed at 1100℃/500h. The other specimens were isothermally solidified. The solidification samples with a size of 5×5×5 mm^3 were cut from the ingots and embedded into graphite blocks with drilling holes. The samples were surrounded by slurry made of alumina powder and silicasol. This packaging can protect melts from flowing out and oxidation effectively during melting and solidification. After desiccation, the graphite blocks were heated to 1420℃ and held for 10 min, followed by cooling at 15 ℃/min to different isothermal solidification temperatures in the range of 1340~1400℃. The samples were held at these temperatures for 10 min followed by water quenching.

The stress rupture life at 1050~1100℃ and 118~147MPa for as-cast shaped specimens was determined. The microstructures of as-cast, heat-treated and stress ruptured specimens were analyzed by SEM, EDS, EPMA, XRD and optical metallography. Electrolytic extraction of minor phases in alloys was performed in a standard 10ml HCl + 90ml methanol + 1g tartaric solution at a voltage of 3~5V for 2h. The volume percent of M_6C in alloys was measured by a standard method of systematic manual point count [9].

Table Ⅰ Analysis Compositions of the Investigated Alloys, wt%

Alloy	Cr	W	Mo	Al	Ti	Nb	Co	C	B	Zr	Ta
1	2.99	17.50	-	6.06	-	0.98	-	0.15	0.022	0.50	-
2	2.98	18.18	-	5.94	-	0.95	2.66	0.074	0.016	0.39	-
3	3.42	17.72	-	5.95	-	1.10	5.04	0.095	0.023	0.49	-
4	3.04	17.30	-	6.24	-	1.00	9.97	0.15	0.02	0.45	-
5	3.00	17.80	-	6.22	-	0.94	-	0.19	0.02	0.49	-
6	2.45	22.00	-	6.10	-	0.89	8.77	0.14	0.02	0.43	-
7	2.98	14.09	1.93	5.61	1.15	2.52	9.93	0.14	0.02	0.10	-
8*	3	14	2	5.5	1.2	4.5	10	0.35	0.02	0.1	-
9	1.31	16.22	2.13	5.96	1.13	0.95	9.63	0.10	0.024	0.121	-
10	1.55	15.46	1.99	5.44	1.31	2.52	9.60	0.14	0.024	0.076	-
11	1.39	16.00	1.99	4.99	1.05	1.04	9.61	0.10	0.045	0.10	6.69
12	1.28	19.20	2.12	5.52	1.10	2.30	14.79	0.05	0.026	0.04	-
13	1.18	14.89	6.32	5.70	1.23	2.40	14.89	0.06	0.022	0.23	-
*Nominal compositions											

Normal and Abnormal Phases

As-Cast Microstructures of Alloys

Normal microstructures of the as-cast Alloy 9, as a representative of high W content alloy, are presented in Figure 1. The microstructures consist of MC carbides, eutectic γ' phase in the interdendritic region and the secondary γ' phase distributing in the γ matrix. Phase analysis results show that Alloy 9 contains 66.2 vol.% γ' phase including about 9 vol.% eutectic γ' phase, 1.2 vol.% MC carbides and minor content of M_3B_2 boride. It is noted that the γ phase is absence in eutectic γ' phase. The results of XRD and metallography indicated that the abnormal phases such as primary M_6C carbides, α (W, Mo) and μ phase could exist in the modified composition alloys.

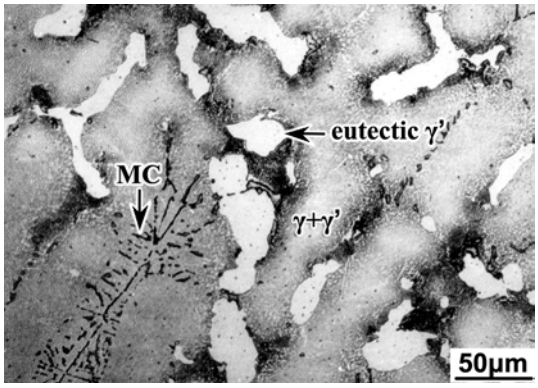

Figure 1. As-cast microstructure of Alloy 9

Primary M_6C carbides

Primary M_6C carbides appear in thirteen alloys listed in Table Ⅰ with different amount, therefore this phase was considered as the most common phase among the abnormal phases. It has been found that primary M_6C carbides exhibited the regularly angular, anchor or bar shapes. M_6C carbides with the angular and bar shapes existed in all alloys and anchor shaped M_6C carbides usually appeared in the alloy containing high levels of W and C, such as Alloy 5 and Alloy 6. Morphologies of primary M_6C carbides are shown in Figure 2. It can be observed that this carbide often coexists with eutectic γ' and possesses size range of 5-~100μm, even maximum size of 0.3mm. The compositions of M_6C carbides determined by EDS in different alloys are represented in Table Ⅱ. It can be seen from this table that M_6C carbides exhibit rather fixed compositions in which levels of (W+Mo) and (Ni+Co) are 73~79wt% and 17~19wt% respectively.

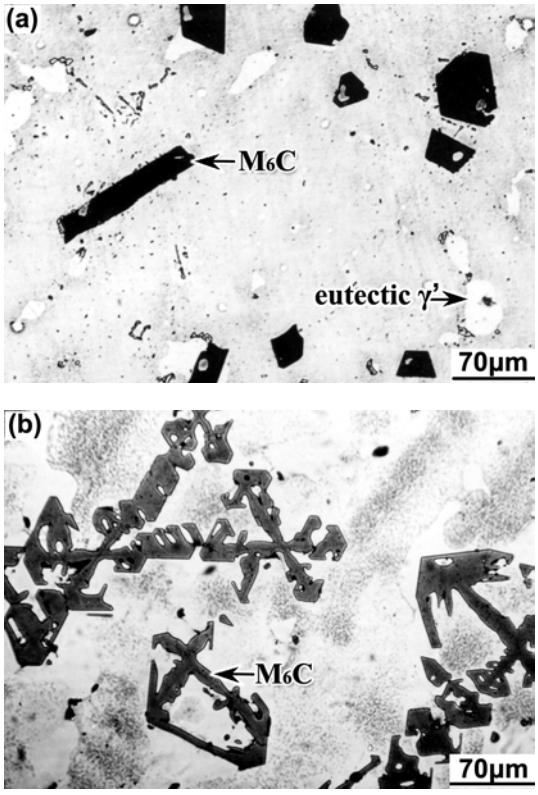

Figure 2. Micrographs of Primary M_6C carbides morphologies: (a) blocky and bar shaped in Alloy 1, (b) anchor shaped in Alloy 5.

Table Ⅱ Composition of M_6C carbides* in various alloys, EDS, wt%

Alloy	W	Mo	Ni	Co	Cr	Nb	Al	Ti	Vickers hardness at 0.49N, GPa
1	77.64	-	17.02	-	2.44	2.19	0.57	-	14.8
5	79.71	-	12.57	4.29	2.07	0.95	0.30	-	15.1
6	79.29	-	12.00	4.77	2.07	1.40	0.43	-	16.7
8	67.52	5.55	14.06	4.54	1.96	5.39	0.44	0.34	15.0
9	71.41	6.53	14.30	4.05	1.00	1.43	0.68	0.60	16.8
*Content of carbon in M_6C is not determined									

M_6C carbide is extremely hard and brittle. This phase has a Vickers microhardness value range of 14.8~16.8GPa at the load of 0.49N listed in Table Ⅱ, but the indentations of hardness cracked at the load of 0.98N.

Primary α (W, Mo) phase

The α (W, Mo) phase existed in Alloy 6 and Alloy 11~13. This phase can be clearly revealed on the polishing surface of metallographic specimen, Figure 3(a). There are two kinds of α phase in different alloys: the dendritic α distributing everywhere, Figure 3(b), and the small bar or blocky α phases only locating in eutectic γ', Figure 3(c). Compositions of α phase were determined by EPMA and are listed in Table Ⅲ. This table indicates that α phase mainly contains elements W, Mo and other elements hardly enter into this phase, hence the phase can be expressed as α (W, Mo). The atomic ratio of Mo/W in Alloy 13 reaches 0.81, but this ratio value in α phase is only 0.27, showing higher tendency of W than Mo for formation of α phase. The Vickers microhardness test at the load of 0.49N was carried out and the average hardness value of 4.52GPa for α phase was obtained.

Table Ⅲ Compositions of α (W, Mo) and μ phase, EPMA , wt%

Alloy	Phase	Ni	Co	Cr	W	Mo	Nb	Ti	Al
11	α	0.65	0.15	0.20	93.45	5.55	-	-	-
12	α	0.31	0.13	0.20	95.13	4.10	0.13	-	-
	μ	17.65	16.92	3.39	44.92	13.71	2.75	0.20	0.50
13	α	0.43	0.15	0.21	86.92	12.11	-	0.18	-
	μ	18.30	17.52	2.94	28.49	28.39	4.35	0.23	0.42

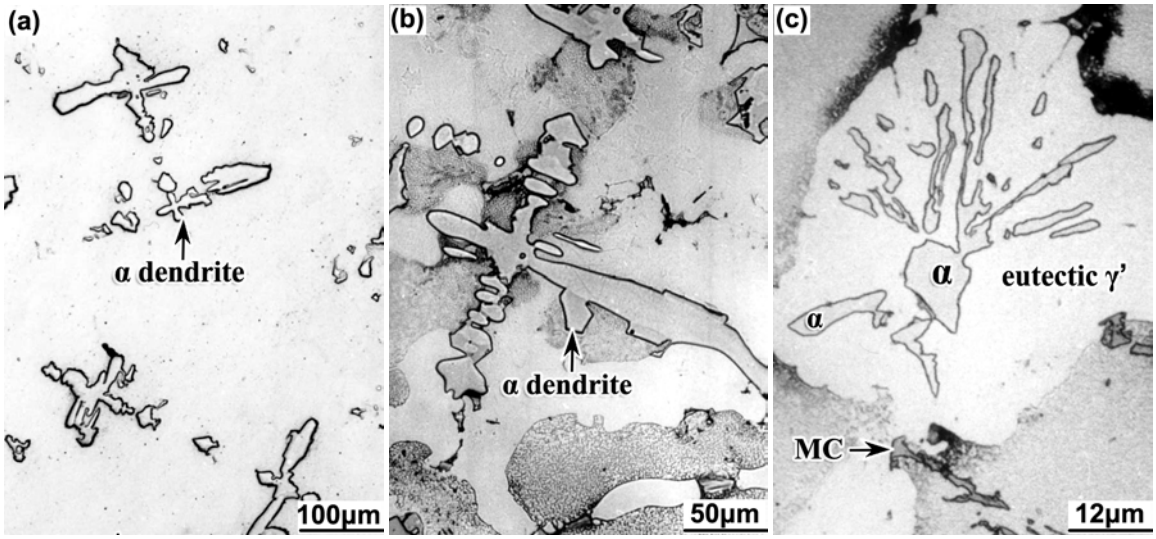

Figure 3. Morphology of α (W, Mo) phases: (a), (b) dendritic shaped in Alloy 6, (c) small bar or blocky shaped in Alloy 11.

Primary μ phase

Figure 4 shows morphology of primary μ phase in Alloy 13. The μ phase can be revealed by electrolytic etching in a H_3PO_4-HNO_3-H_2SO_4 solution, Figure 4(a), and this phase is tinted as dark blue tone by soaking at 450℃/30min making sharp black and white contrast, Figure 4(b). The primary μ phase normally appears in the periphery of eutectic γ'.

The EPMA results in Table Ⅲ demonstrate that the elements of Mo, W, Cr, Nb and Co are μ –formers. Based on atomic percent, contents of the above mentioned elements in μ phase are much higher than those in the alloy, especially the total amount of refractory elements (Mo + W + Cr + Nb) in μ phase is as high as 44~47 at% which is three times higher than that of the alloy.

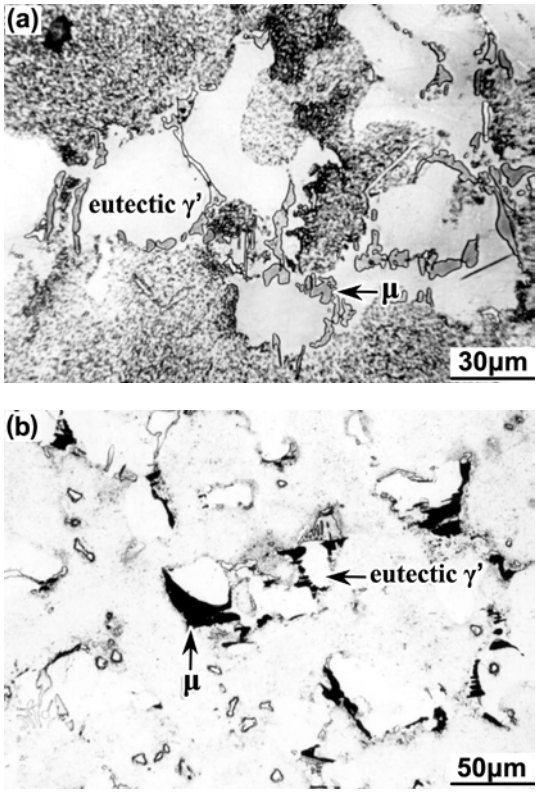

Figure 4. Primary μ phase in Alloy 13: (a) etching by mixed acid, (b) tinting.

Precipitation Conditions of Abnormal Phases

Primary M_6C carbides

Metallographic experiments certified that susceptibility of the formation of M_6C carbides was very different in various sections of the same casting or in different heats of alloys with same composition. For example, as specimen of Alloy 10 with M_6C was heated to 1420℃ and poured into metal chill mold, M_6C was eliminated, Figure 5 (a). In contrast, large amount of M_6C formed in ordinary M_6C-free specimen due to the remelting and slow furnace cooling, Figure 5 (b). Isothermally solidified experiments of Alloy 9 proved that long bar-shaped M_6C carbides formed as shown in Figure 6 at 1375℃ which was 20℃ higher than that of MC formation, and this precipitation could last until 1340℃. Once primary carbides form, the quantity of MC will decrease obviously. It is evident from the above results that the formation of M_6C is closely related to the cooling rate of solidified process and the rapid solidification can prevent from precipitation of M_6C. Since dendtitic spacing was considered as a characterizing parameter of cooling rate during solidification of castings, a relationship between the dendritic spacing and the volume fraction of M_6C carbide was measured for seven alloys, shown in Figure 7. This figure indicates that M_6C does not present in the thinner sections of specimens with dendritic spacing less than 50μm, except for the high carbon content Alloy 8.

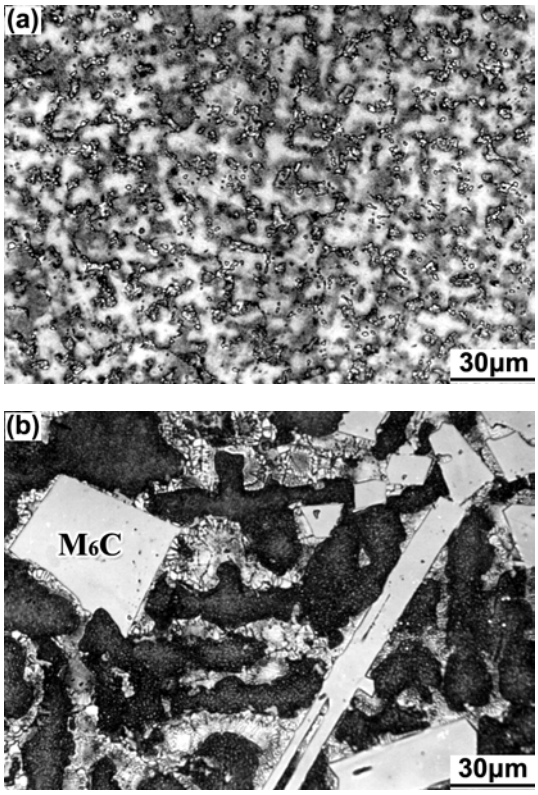

Figure 5. Tendency to form M_6C carbide for Alloy 10: (a) rapid cooling in cold metal mold after remelting, (b) furnace cooling after remelting.

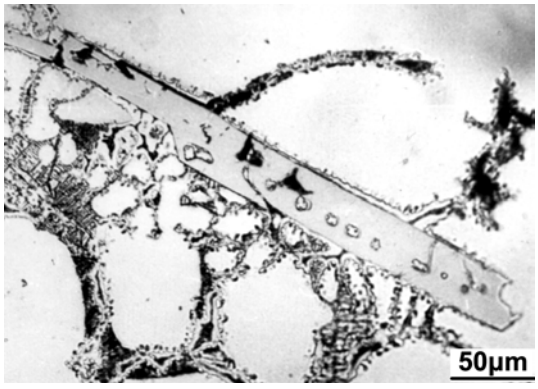

Figure 6. Long bar-shaped M_6C carbide precipitated in Alloy 9 after treatment of 1420℃/10min+1375℃/10min+water quenching.

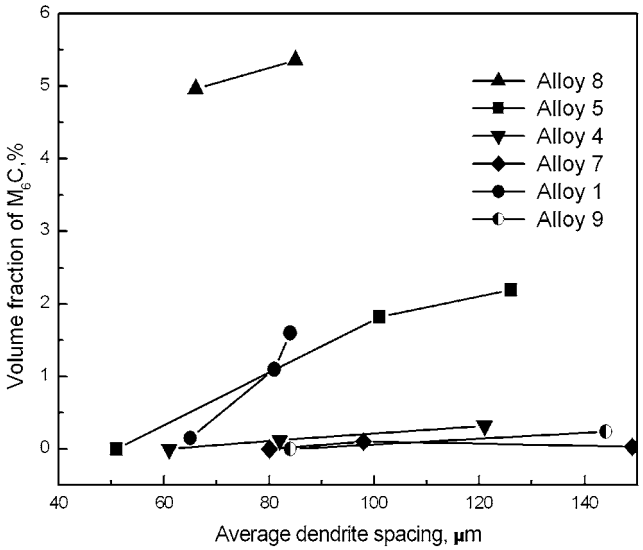

Figure 7. Relationship between the dendritic spacing and the volume percent of M_6C carbides.

It can be seen from Figure 7 and Table Ⅰ that elements W, Mo and C are strong M_6C-formers and primary M_6C carbides easily form as the amount of (W + Mo) and carbon is over 18wt% and 0.15wt% in as-cast alloys respectively.

Element Co and Ru are effective retarders of M_6C. Accompanied by an increase of the Co content in alloys, the volume percent of primary M_6C decreases significantly, Figure 8. Addition of 10-15 wt.% Co is necessary to stabilize the microstructure of superalloys containing high W content. The element Ru is even stronger than Co in retarding the formation of M_6C phase. Large amount of primary M_6C existed in DTA specimen of Alloy 9 cooled down at the rate of 10℃/min. However, no M_6C appeared in DTA specimen of Alloy 9 with 3 wt.% Ru at the same cooling rate, even though the Ru-bearing specimen was soaked for 10min at 1370℃ which is the sensitive temperature of M_6C formation.

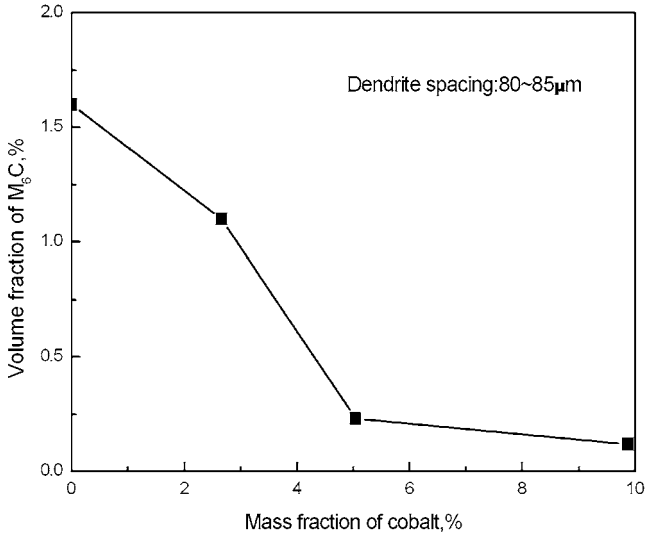

Figure 8. Relationship between the Co content and the volume percent of M_6C carbide in Alloy K9.

Primary α (W, Mo) and μ phases

The α (W, Mo) dendrites shown in Figure 3 (a) and (b) formed at very onset of solidification in the alloys with the content of (W + Mo) higher than 20 wt%. It was demonstrated by solidified experiment that for Alloy 6, the beginning formation of γ dendrites took place at 1380℃, whereas primary α (W, Mo) dendrites formed at 1385℃, Figure 9. The similar α–W dendrite in the Ni-W eutectic alloy was reported [11].

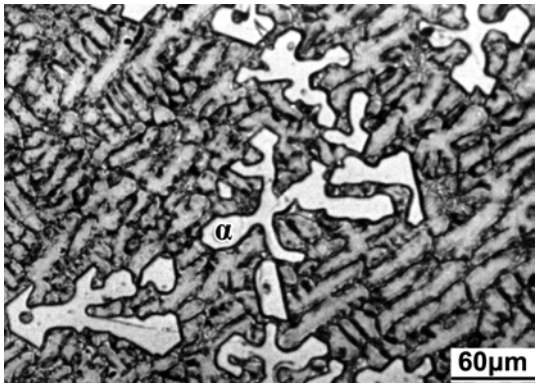

Figure 9. α (W, Mo) dendrites precipitated from liquid Alloy 6 after 1420℃/10min+1385℃/10min and very fine γ dendrites formed by quenching.

The small bar shaped α (W, Mo) phase within eutectic γ' shown in Figure 3 (c) is due to high content of Ta in Alloy 11. As a strong positive segregation element and γ'-former, Ta raises the volume percent of eutectic γ' up to 20 vol.%, whereas the solubility of W in eutectic γ' is far lower than that in γ phase. During the formation of eutectic γ', the excess W precipitates in the form of α (W, Mo) solid solution.

In alloys containing lower than 0.06 wt% C and higher than 18 wt% (W+Mo), primary μ phase often appears, especially in alloys with Mo higher than 4 wt%. The precipitated reactions of eutectic (γ +γ') and MC carbide basically finish at 1270℃ for Alloy 13, and the residual liquid which rich in W, Mo and poor in Al, C is beneficial to form μ phase.

Transformation of Abnormal Phases

M_6C carbide is the most stable phase in the three abnormal phases. Once this phase formed, it is impossible to be removed in a solid state. In contrast, the α and μ phases can transform into M_6C carbides during long-term thermo-exposure or treatment of solid solution.

Transformation of α (W, Mo) Phase

Figure 10 represents the evidence of α transformation. After thermal exposure of 1100℃/500h, a large part of MC carbide decomposed and an appreciable amount of carbon promoted the reaction of α +C→M_6C. Therefore all small bar shaped α phase fully transformed into M_6C carbide and large blocky α only transformed partially, Figure 10(a). Indentations of microhardness at the load of 0.49N in transformed and untransformed regions are shown in Figure 10(b), and the hardness values and EDS compositions of the two regions are given in Table Ⅳ, in which

compositions of some granular and plate M_6C are also listed. The bar shaped α phase within eutectic γ' for Alloy 11 slowly resolves and agglomerates into the spherical particles enveloped by γ phase during a solid solution treatment above 1260℃. This change is more distinct at a treatment of 1290℃/3h, shown in Figure 9(c).

Table Ⅳ Compositions of M_6C* carbides and α phase in Alloy 11 after 1100℃/500h thermal exposure, EDS, wt%

Phase	Al	Ti	Cr	Co	Ni	Nb	Mo	W	Ta	Vickers hardness, GPa
Granular M_6C	0.08	0.06	1.64	9.44	18.23	0.95	10.30	57.66	1.60	-
Plate M_6C	0.51	0.14	1.27	8.71	21.80	0.40	6.75	59.31	1.59	-
M_6C transformed from α	0.16	0.07	1.54	9.28	15.36	0.00	6.11	68.90	0.00	10.6
Residual α (W, Mo)	0.04	0.01	0.26	0.52	2.93	0.00	6.13	88.88	1.68	5.3
*Content of carbon in M_6C is not determined										

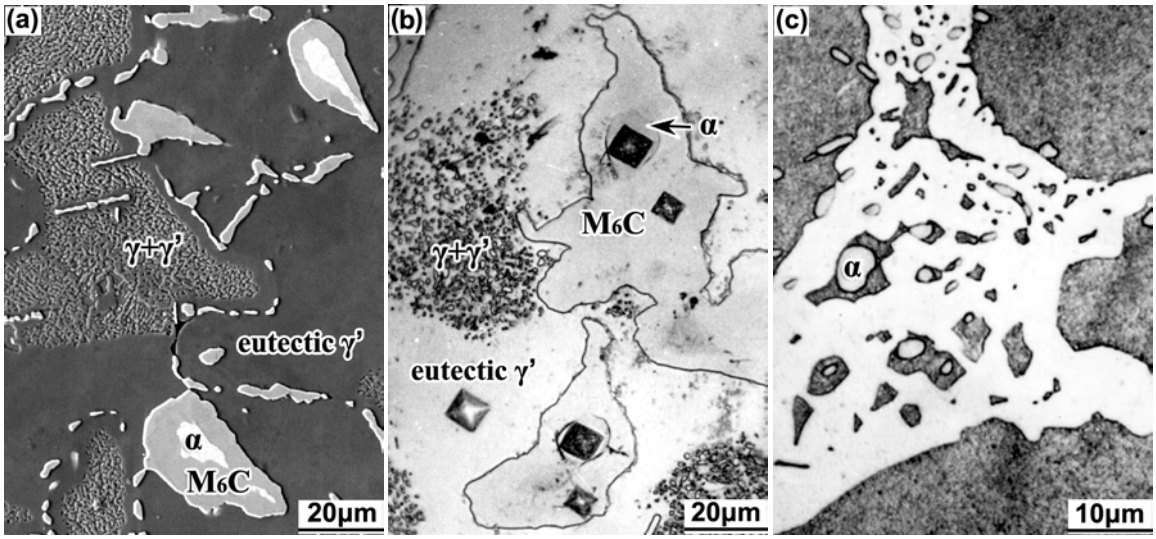

Figure 10. Transformation and resolution of α phase in Alloy 11: (a) and (b) 1100℃/500h, (c) 1290℃/3h.

Transformation of μ Phase

Primary μ phase is rather stable below 1100℃ and only a few of plate μ phase at periphery of eutectic γ' phase resolves and changes into small blocky phase surrounded by γ phase after thermal exposure of 1100℃/500h for Alloy 13, Figure 11(a). As temperature approaches 1200℃, the μ phase became very unstable and transformed to M_6C. Figure 11 (b) illustrates the microscopic appearance of μ phase dissociating to M_6C after treatment of 1230℃/30min for this alloy. It can be seen from Figure 11 (b) that the ordinary μ surrounding γ' phase changes partially to regularly angular M_6C and residual μ phase coarsens and still maintains irregular shape. After 1230℃/2h, no μ phase exist in the alloy. The μ and M_6C compositions were measured by EPMA and presented in Table Ⅴ. These data indicate that the M_6C transformed from μ contains a higher W content and lower Ni, Co, Cr and Mo contents, as compared with residual μ phase.

Table Ⅴ Compositions of residual μ and M_6C transformed from μ phase in Alloy 13 after treatment of 1290℃/30min, EDS, wt%

Phase	Ni	Co	Cr	W	Mo	Nb	Al	Ti
μ	22.61	15.56	2.64	27.11	28.61	2.29	0.75	0.43
M_6C*	14.31	5.59	0.84	58.24	17.37	1.78	0.96	0.55
*Content of carbon in M_6C is not determined								

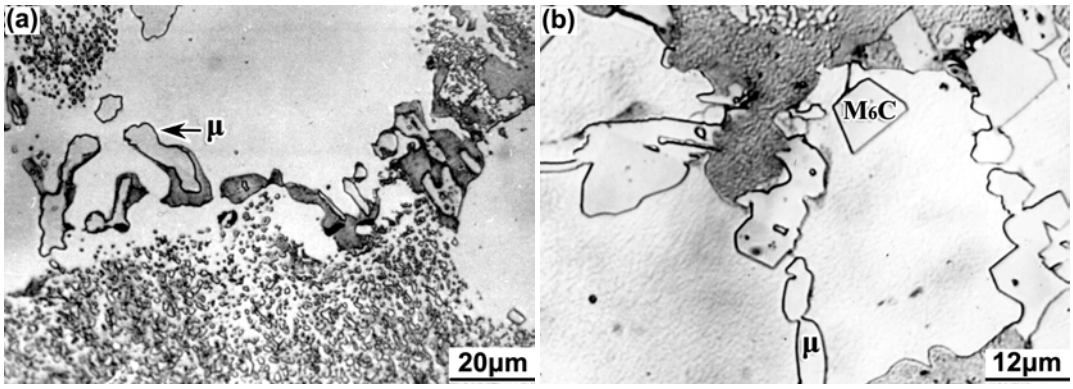

Figure 11. Resolution and transformation of μ phase in Alloy 13: (a) thermal exposure of 1100℃/500h, (b) solid solution of 1230℃/30min.

Effect of abnormal phases on stress rupture life

Figure 12 portrays the average stress rupture life of test bars at 1050℃/147MPa, 1080℃/118MPa and 1100℃/118MPa. All of the low life alloys, such as Alloy 6 and 10-1, contain more than 1.5 vol.% primary M_6C. Alloy 10-1 and 10-2 belong to the same master alloy, but different cast processing. M_6C-free Alloy 10-2 has a rupture life of 89.5h at 1080℃/118MPa due to rapid cooling during remelting and pouring, whereas the stress rupture life of Alloy 10-1 is only 16.7h because of the formation of large amount of M_6C during slow cooling solidification. Similarly, as compared with the cast shaped test bars, the temperature capability of Alloy 1 decreases about 40℃ in the M_6C-containing specimens cut from heavy sections with a 80mm diameter.

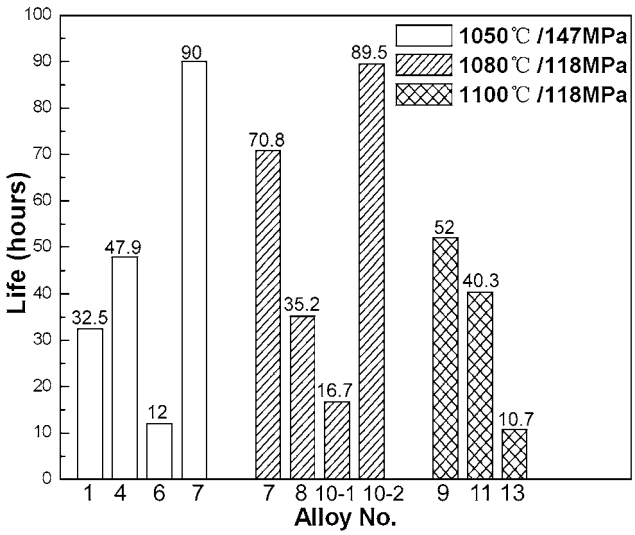

Figure 12. Stress rupture life of alloys at different temperatures and stresses.

Metallographic observations proved that cracks generally occurred at interface of M_6C/matrix, as pointed by arrows in Figure 13(a). The initiated cracks propagated as cavities during stress rupture test, Figure 13(b).

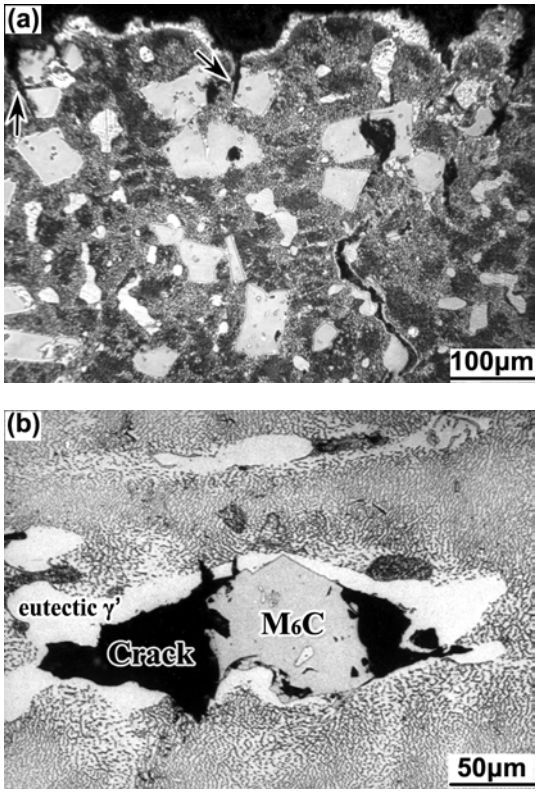

Figure 13. Stress rupture cracks deduced from primary M_6C: (a) in specimen of Alloy 8 ruptured at 1080℃/118MPa for 32.5h, (b) in specimen of Alloy 9 ruptured at 1100℃/118MPa for 35.4h.

An appreciable amount of μ phase in alloys will degrade mechanical properties significantly. Low stress rupture life of Alloy 13 in Figure 12 is associated with μ phase existence in great quantity. Small amount of α (W, Mo) phase has no obvious effect on stress rupture life of alloys. For instance, Alloy 11 containing bar like α phase in large parts of eutectic γ' still possessed a 40.3h rupture life.

Discussion

It was found that Alloy K9 was a forging die material suitable for application below 1050℃. Alloy 601 is a promising candidate due to a 20℃ higher temperature capability than that of K9 and a very good stability of microstructure in the temperature range of 850~1100℃ [12]. However, it is noteworthy that these alloys exhibit a high sensitivity of microstructure and mechanical properties to alloy composition and conditions of solidification, especially a great number of primary M_6C carbides easily form in Co-free Alloy K9 cast forging die with a section size over 200mm, similar section size effect of cast blades was concerned as early as 1970's and stress rupture properties of blades at different sections were measured [13]. For large size dies as heavy as tons, it is impossible to directly take specimens from die to inspect microstructure and mechanical properties. A reasonable solution is to modify the compositions of alloys in order to obtain a wide tolerance for cast variation. This study satisfied the above demands basically.

At the end of 1970's, the shortage of Co in international market promoted development of low Co or Co-free cast superalloys [14, 15]. These alloys have almost the same strength level as their Co-containing counterparts at elevated temperature. In fact, All of the Co-bearing and Co-free Alloy K9 possess the similar stress rupture life at 1050℃/147MPa due to no M_6C existing in cast shaped test bars, as compared between Alloy 1 and Alloy 4 in Figure 12. Thus Co-free Alloy K9 was selected to be the forging die material due to low cost consideration. Afterwards, when this alloy was utilized to cast large size die, cracks were difficult to avoid because of large quantities of M_6C carbides formed in heavy section castings. Through this study, it is recognized that element Co is an effective retarder of primary M_6C; therefore, 10wt% Co content for cast die alloy is necessary to prevent embrittlement caused by M_6C.

In Alloy K9 with 0.15wt% C, even though 10wt% Co has been added, about 0.32 vol.% primary M_6C still formed in 20×20mm square cast bars. Therefore it is indispensable to further decrease the content of carbon. As followed Alloy 601, carbon content was controlled as to be 0.10wt%. The complement result showed that despite the carbon content decreases to 0.05wt%, Alloy 601 still maintained a 46h rupture life at 1100℃/118MPa. In fact, many low carbon alloys such as CM247LC and CM186LC exhibited superior mechanical properties and were widely applied to gas turbine blades [16, 17]. Hence for large section castings, carbon content of alloys should be in the range of 0.04~0.07wt%.

Conclusions

1. Cast nickel base superalloys high in W content are suitable for casting high temperature dies. When compositions and cast processing are not controlled reasonably, three abnormal phases: primary M_6C carbides, α (W, Mo) and μ phase will form. Especially M_6C deteriorates the high temperature strength of the alloys remarkably.

2. The primary M_6C carbides begins to form from liquid at 1375℃ and lasts to precipitate until the eutectic γ'. Rapid cooling through solid-liquid temperature range can restrict M_6C formation. As interdendritic spacing in castings is less than 50μm, no M_6C forms. However large blocky M_6C appears in a heavy sections possessing interdendritic spacing higher than 150μm.

3. It is very easy to precipitate primary carbides in alloys containing more than 18wt% (W+Mo) and 0.15wt% C. 10wt% Co or 3wt% Ru can effectively retard the formation of M_6C. Although carbon content below 0.05wt% decreases M_6C precipitation sensitivity significantly, promotes the formation of primary α (W, Mo) and μ phase. Therefore it is preferred to maintain 0.04~0.07wt% C and 10~15wt% Co in alloys.

Acknowledgment

This project (contract No. 50371004) was supported by the National Natural Science Foundation of China.

References

1. W. J. Waters and J. C. Freche, "Nickel-base Alloy with Important Strength at 2000 to 2200 F," *Met. Eng. Quart.*, 10 (2) (1970), 55-60.
2. W. J. Waters and J. C. Freche, "NASA Vane Alloy Boasts High Temperature Strength," *Met. Prog.*, 1975, No.3: 57-61
3. S. W. K. Shaw and P. J. Penrice, "Nickel-Chromium-Tantalum Alloys," U. S. Patent No.3617262, 2 November 1971.
4. S. Tin, T.M. Pollock and W.T. King, "Carbon Additions and Grain Defect Formation in High Refractory Nickel-Base Single Crystal Superalloys," *Superalloys 2000*, ed. T.M. Pollock et al. (Warrendale, PA: TMS, 2000), 201-210.
5. H. Harada, H. Murakami, "Design of Ni-Base Superalloys," *Computational Material Design, Springer*, ed. T. Saito (Berlin: Springer, 1999), 39-67
6. Y. Zheng and Y. Han, "Cost Considerations of Single Crystal Superalloys for Gas Turbine," *Acta Metallurgica Sinica*, 38 (12), (2002), 1203-1209.
7. Editorial Committee of China Aeronautical Materials Handbook, *China Aeronautical Materials Handbook*, vol. 2, (Beijing: Standards Press of China, 2002), 792-795.
8. Y. Zheng, "Development and Application of Low Cr and High W Content Cast Nickel Base Superalloys in China," *Journal of Aeronautical Materials*, Special Issue for Celebrating Aviation's 100, (2003), 227-232.
9. R. F. Allen et al., "Test Method for Determining Volume Fraction by Systematic Manual Point Count," Annual Book of ASTM Standards 2000, vol. 03.01, Designation E562-99 (West Conshohocken, PA: ASTM, 2000), 535.
10. C. T. Sims and W. C. Hagel, *The Superalloys* (New York; John wiley & Sons, 1972), 479.
11. W. Kurz and B. Lux, "On the Growth of the Ni-W Eutectic," *Met. Trans.*, 2 (1971), 329-330.
12. L. Zheng et al., "Microstructure and its Stability of a Cast Nickel Base Superalloy containing Low Level of Cr and High Level of W," *Journal of Aeronautical Materials*, 24 (1) (2004), 17-21.
13. C. H. Lund, J. Hocking and M. J. Woulds, "Casting Process for Nickel Base Alloys," U. S. Patent No. 3677331, 18 July 1972.
14. M. V. Nathal, R. D. Maier and L. J. Ebert, "The Influence of Cobalt on Microstructure of the Nickel-Base Superalloys Mar-M247," *Metall. Trans (A)*, 13A (1982), 1775-1783.
15. Y. Koizumi, M. Yamazaki and H. Harada, "Development of

Cobalt-free Nickel-base Superalloys," *Transactions of National Research Institute for Metals*, 22 (3) (1980), 32-38.

16. K. Harris et al., "Development of the Rhenium Containing Superalloys CMSX-4 & CM186LC for Single Crystal Blade and Directional Solidified Vane Applications in Advanced Turbine Engines," *Superalloys 1992*, ed. S. D. Antolovich et al. (Warrendale, PA: TMS, 1992), 297-306.
17. M. Maldini et al., "Creep and Fatigue Properties of a Directionally Solidified Nickel Base Superalloy at Elevated Temperature," *Superalloy 1996*, ed. R. D. Kissinger et al. (Warrendale, PA: TMS, 1996), 327-334.